UNIVERSITY OF CAPE TOWN
Department of Electrical Engineering

EEE3094S – Control Engineering
Altitude Autopilot
2019 S2 Report

Dylan muller

1/09/2019

Declaration

1. I know that plagiarism is wrong. Plagiarism is to use another's work and pretending that it is one's own.

2. I have used the <IEEE> convention for citation and referencing. Each contribution to, and quotation in, this report from the work(s) of other people has been attributed, and has been cited and referenced.

3. This report is my own work.

4. I have not allowed, and will not allow, anyone to copy my work with the intention of passing it of as their own work or part thereof.

Name:.....Dylan..... Student Number: MLLDYL002

Signature:... DM.....

Date:.....1/09/2019.....

Executive Summary

Control system design is an integral part of the modern-day engineering industry and its implementation may be found in a wide variety of commercial products whose performance depends on some type of output control.

The aim of this project is the design and implementation of a suitable control system for a derived helicopter model.

Specifically, an altitude autopilot system shall be synthesized and characterized using classical design procedures as well as CAD assisted tools such as MATLAB to verify model accuracy.

Finally, the controller model is to be implemented using a simple analogue computer made up of operational amplifiers.

Contents

1. Introduction and Background on Helicopter Control (pg 1.)
2. Technical Specifications (pg 2.)
3. Modeling, System Identification and Problem Formulation (pg 3.)
4. Controller Design and Simulation (pg 5.)
5. Controller Implementation (pg 8.)
6. System Testing (pg 9.)
7. Conclusion (pg 10.)

1. Introduction and Background on Helicopter Control

Our system under consideration is based off a mathematical model of an aerodynamic vehicle, a helicopter.

A hardware simulator implementing the model, with a software graphical user interface (GUI), was used to simulate the real-time aerodynamic behavior of the system using parameters such as rotor thrust, pitch, gravity as well as respond to input/output state changes.

Table I. summarizes the various input and output ports available on the simulator as well as a description of their corresponding model dynamics and output representation.

Type	Port	Simulated Dynamic	Representation	Range/V
Input	**A2**	▪ Rotor pitch ▪ Magnitude and direction of thrust (m/s)	Input control voltage	0-5 2.5 = 0 deg pitch (stabilized)
Output	**D0**	▪ Current altitude (m)	Output voltage	0-10

Table I. Summary of hardware simulator.

By adjusting the relevant port A2 control voltage, the helicopter could be directed upwards, downwards or stabilized (2.5V input).

However, adjusting this manually to obtain a desired altitude setpoint is difficult for a human operator, defined by large response times and error, and thus a more efficient means of altitude control is necessary.

Our user would ideally prefer to simply set the desired altitude and initiate the control system. Therefore, a fast response time, good setpoint accuracy and smooth setpoint transition are important for our user. Component cost and count should also be taken into consideration to produce a cost-effective system for our user.

A simplified use case diagram for the required system is depicted in **Figure 1**.

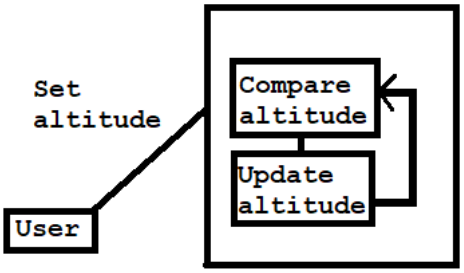

Figure 1. Use case diagram of system.

2. Technical Specifications

Given our user requirements, a technical evaluation of the requirements is thus necessary, we shall refer to the system in question as our plant and compensator as our controller.

Firstly, a form of feedback is necessary, whereby our current altitude may be continuously compared with that of the setpoint.

Two forms of feedback exist, positive and negative. Negative feedback produces a stabilizing action which is what we require, where a portion of the output may be looped back to a differential summer and the relevant corrective control actuation produced to the input of the plant in a manner determined by the controller.

This is the basis of the classic negative feedback control system depicted in **Figure 2**.

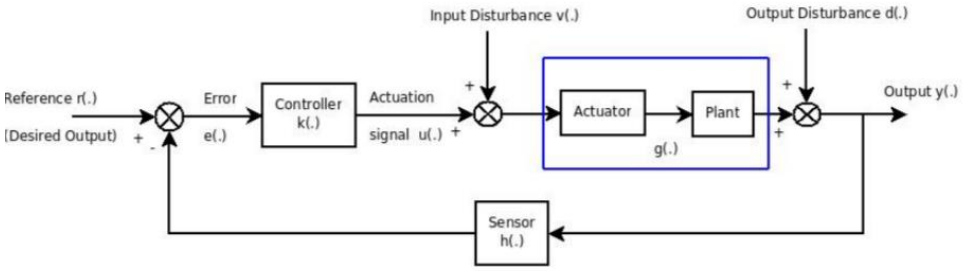

Figure 2. Negative feedback control system

Various performance quantifiers exist for control systems and system performance may be characterized both in the temporal and spectral domain.

Table II. summarizes various performance metrics and requirements for our closed loop control system (treated as a second order dynamic system)

Parameter	Description	Description	Requirements Analysis
$g_{vy}(s)$, $g_{dy}(s)$	Disturbance and noise rejection	Transfer functions relating output for noise step inputs.	Project requirements were 5% within setpoint. Should be within %PO
A±2%	Steady state error	Deviation from the final steady state setpoint.	Project requirements were 5% within setpoint.
t±2%	Settling time	Time taken to reach 2% within steady state value.	Should be no longer than half of the first order plant. Plant requires finite response time. Reduction in t increases design complexity/tradeoff.
ζ	Damping ratio	Rate of oscillation decay for second order system.	ζ ≥ 0.3 A damping ratio > 0.3 is a universally accepted minimum for electrical systems. We would like to operate above the minimum.
%PO	Percent overshoot	Max overshoot as a percentage of the steady state value. For transient tracking and disturbance response.	%PO < 16.3% ~ 20% May be derived from damping ratio for second order systems.

Table II. Controller performance metrics.

The performance metrics defined in Table II. ensure that our user requirements for a fast and smooth setpoint transition are met and that control action is not underdamped, oscillatory or in general unsafe in nature.

3. Modeling, System Identification and Problem Formulation (****sensor gain)

As mentioned above, it was necessary to use feedback control to improve our plant. An analytic analysis of the closed loop response requires that the plant transfer function be available.

Multiple ways of deriving a plant transfer function exist, namely through state space ('white box') modelling or the so called 'black box' modelling approach which involves injecting a unit step into the input port of the device under test (DUT) and analyzing the response from which various parameters characterizing the plant may be derived.

For this project, the latter approach, i.e black box modelling, was used to characterize the plant transfer function.

The simulator software GUI provided a faculty for recording the altitude outputs (physical representation in meters and output voltage) as a function of the input control voltage.

Initial conditions for black box modelling need to be taken into consideration, specifically it was determined that a 2.5V initial state at port A2 be applied before stepping our input (up to 5V), this is due to the fact that modelling of the system needs to be done from a resting state, since the goal of the controller should be to provide corrective action only when our setpoint altitude differs from our actual altitude and not during a setpoint match, during which the A2 input port should be at 2.5V - representing 0 degrees rotor pitch or, more directly, a 0 net thrust state (hovering action).

The procedure consisted of applying a unit step into port A2 (2.5 to 5V) of the simulator by short circuit to a 5V reference potential (**Figure 3**) and consequently recording port data which was exported to a CSV file for analysis.

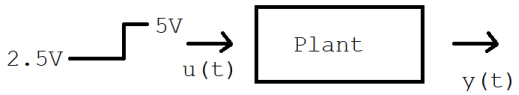

Fig 3. Short circuit unit step input (black box characterization)

Recording length was deemed suitable when the rotor thrust parameter indicated on the software GUI was reduced to approximately zero, this is because the function of our plant model is to characterize the relationship between control action and net thrust/vehicle velocity and since net thrust is eventually reduced to zero/constant vehicle velocity, the point of minimum influence on our model is obtained and we may stop collecting data.

This procedure was repeated approximately three times to enhance the accuracy of the final plant model by averaging.

The processed output response, of vehicle velocity versus time of the third test is indicated in **Fig 4**.

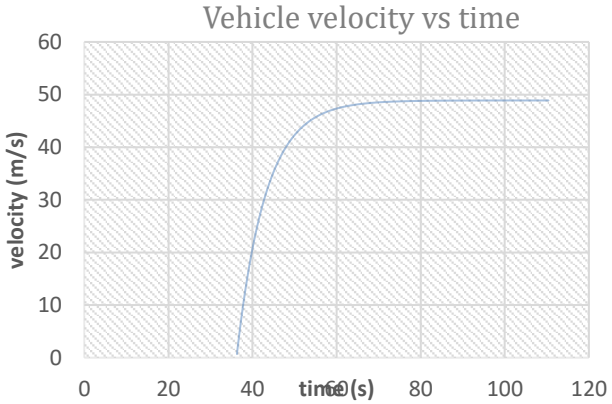

Fig 4. Vehicle velocity as a function of time.

As may be observed the response is characteristic of a first order system with a dynamic characteristic defined as follows (**Figure 5**):

$$g(s) = \frac{A}{\tau s + 1}$$

Figure 5. First order response characterization.

Where τ, the time constant, represents time taken to each 63.3% of the final DC value and A represents the DC gain defined as follows (**Figure 6**.):

$$A = \frac{y_f(t) - y_i(t)}{u_f(t) - u_i(t)} = \lim_{s \to 0} g(s)$$

Figure 6. DC gain equation.

$y_f(t)$- $y_i(t)$ representing the difference in the final and initial dc states and $u_f(t)$- $u_i(t)$ representing the step input size which is 2.5V.

Values obtained for **τ** and **A** for each set of readings were as follows, care was taken to obtain accurate readings (**Table III**.):

#	**A**	**τ / s**
1	19.5518	6.8815
2	19.5520	6.8817
3	19.5522	6.8816
Avg	19.552	6.8816

Table III. Values obtained for each set of readings.

This leads to the construction of our first order plant transfer function (**Figure 5**) by substitution (**Figure 6**).

$$g(s) = \frac{19.552}{6.8816s + 1}$$

Figure 6. First order open-loop derived plant transfer function.

The first order open loop transfer function contains at pole at **s = -0.1453** indicating stability.

However, since the control system is operating in closed loop according to an altitude setpoint rather than a strict velocity setpoint our plant model needs to be expressed in terms of the Laplace equivalent of the temporal position vs time relation.

Position as a function of time may be expressed as the integral of velocity. Conveniently integration in the Laplace domain may be expressed by multiplication with a $\frac{1}{s}$ term (known as the integrating term).

If we apply the integration term to our first order derived plant model, we obtain a second order positional model defined as follows (**Figure 7**):

$$g2(s) = \frac{19.552}{6.8816s^2 + s}$$

Figure 7. Second order closed loop derived plant transfer function.

The system indicated in **Figure 7** has its poles located at **s = 0** and **s = -0.1453** indicating marginal stability. A closed loop system, simply consisting of $g2(s)$ was simulated in MATLAB and the results indicated in **Figure IVA.**

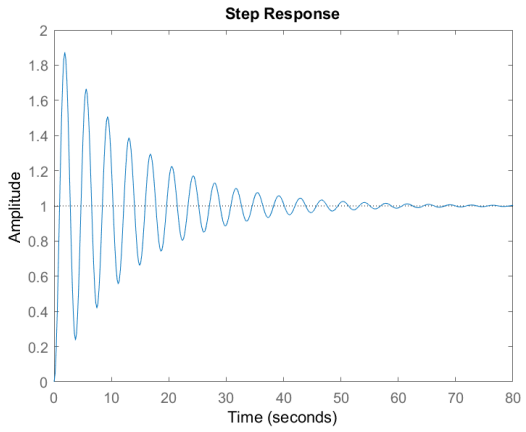

Figure 8. Closed loop response of g2(s) without controller

The closed loop stability component may be observed due to the presence of damping, however settling time for the system is large > 60s as well as overshoot which is impractical. We have formed a crude feedback system by directly connecting the output to the input.

This highlights the importance of the controller block k(s), whose purpose is to change the location of poles to produce a more stable system response, one that should meet our user requirements as mentioned above.

4. Controller Design and Simulation

Following system identification, a suitable controller is needed to improve the system response observed in **Figure 8.**

One approach to the design of a suitable controller $k(s)$ entails an analysis of the pole and zero positions of the plant and how they may be manipulated by a suitable controller. Given the closed loop transfer function of a control system relating the input reference to the output:

$$g_{CL}(s) = \frac{y(s)}{r(s)} = \frac{gk(s)}{1 + hgk(s)}$$

The characteristic polynomial may be extracted from $g_{CL}(s)$:

$$D(s) = 1 + q(s) = 1 + hgk(s)$$

Where $q(s)$ represents the open loop transfer function and $h(s)$, the sensor gain. It is known that $D(s)$ influences the response of the closed loop system, characterizing system stability, output and speed.

The root locus is then defined as a plot of the pole and zero positions of the characteristic equation of $D(s)$ written in its monic form, as the value of γ (defined as the root locus gain) is varied. :

$$D(s) = 0 = 1 + q(s) = 1 + \gamma \frac{N_q^*(s)}{D_q^*(s)}$$

Depending on the pole/zero transition requirement different controller types may be more or less suitable.

The procedure is as follows: identify pole/zero location requirements, identify a suitable effector (i.e pole attractor, repeller) $k(s)$, find monic $q(s)$ and solve for the required root locus gain (γ) for pole/zero placement.

Figure 2. is a manifestation of the most basic controller type, namely the proportional controller, which simply acts to increase or decrease root locus gain, in essence the γ term of monic $D(s)$ may be viewed as the proportional controller $k(s)$ or the 'P' term.

The root locus may then be defined in the most basic sense as a plot of the pole/zero changes as the gain of the proportional controller is varied. Most controllers have some form of gain and thus a proportional component often donated P.

The monic polynomial $D(s)$ of the closed loop transfer function $g_{CL}(s)$ of plant $g2(s)$ is as follows:

$$D(s) = 1 + \left(\gamma \frac{A}{\tau}\right) \frac{1}{s(s + \frac{1}{\tau})} = 1 + \left(\gamma \frac{19.552}{6.8816}\right) \frac{1}{s(s + \frac{1}{6.8816})}$$

From which the root locus may be derived following $D(s) = 0$ (solution to characteristic equation) with: $\gamma \in (-\infty, \infty)$:

$$D(s) = \frac{-\frac{1}{\tau} \pm \sqrt{\left(\frac{1}{\tau}\right)^2 - 4(1)(\frac{A}{\tau}\gamma)}}{2(1)} = \frac{-\frac{1}{6.8816} \pm \sqrt{\left(\frac{1}{6.8816}\right)^2 - 4(1)(\frac{19.552}{6.8816}\gamma)}}{2(1)}$$

Using MATLAB control system designer, it is possible to visualize the root locus (**Figure 9**):

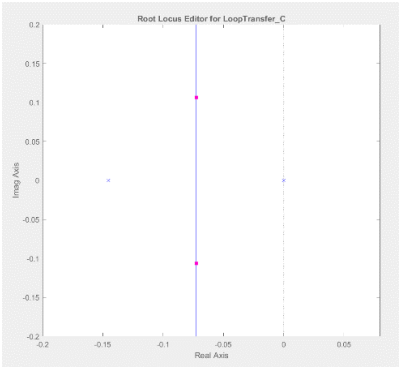

Figure 9. Root locus plot of $g_{CL}(s)$

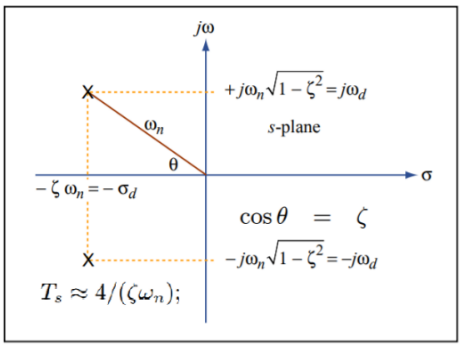

Figure by MIT OpenCourseWare.

Figure 10. Second order system parameter derivations from root locus.

As the value of root locus gain is increased the two poles are seen attracting, until branching occurs at the centroid of the two poles.

Properties such as damping ratio ζ damping frequency ω_d, percent overshoot %PO, settling time t±2% as well as a variety of other important parameters pertaining to second order systems may be determined through an analysis of the root locus for a given closed loop transfer function $g_{CL}(s)$

A brief overview of the various parameters and their relation to the root locus is summarized in Figure 3.

It may be observed that the damping ratio ζ decreases as the angle subtended by a ray drawn from the origin to the pole location increases in angle. Thus, for a high damping ratio requirement, it is desirable to operate at a distance not too far up the j ω axis which also quantifies the magnitude of the natural damped frequency ω_d.

We shall now proceed with a design of a proportional controller to try and meet the performance criteria defined in Table II.

Empirically it has been determined that a high damping ratio (ζ > 0.7071) is desirable for many control system types. A high damped ratio decreases percent overshoot %PO and system 'stress'.

This translates to an angle restriction of $\theta < \cos^{-1}(0.701) = 45°$ on the root locus.

A **τ** of approximately 6.88s was obtained for our plant model and thus our settling time requirement is translated into **t±2%** < ~ 3s

However, given the relation of t±2% to $\zeta\omega_n$ (**Figure 10**) a minimum ω_n magnitude of 1.89 (traced as a circle around the origin) is required (ζ = 0.7071) for which roots cannot reside within to meet the settling time specifications. Since the furthest root resides at **-0.1453** at γ = 0 and given our root locus angle restriction of $45°$ a proportional controller will not satisfy a key criterion of our control system and is therefore unsuitable.

In the design of a suitable controller for our plant $g2(s)$ we are required to develop a controller function k(s) to adequately effect/shift our poles to a suitable location on the root locus, satisfying our user requirements completely.

Our two main limiting factors are thus the settling time requirement and damping ratio, we proceed using the pole placement synthesis method.

Choose **ζ = 0.9, t±2 = 1s**. therefore, **s=-4.0 +- 1.9j** is a suitable desired pole location.

The total phase addition required is given by (modified angle criterion),

$$\theta_t = 180 - angle\big(\mathrm{q} * (\mathrm{so})\big) = 180 - \text{angle}\left(\frac{19.552}{6.8816 * (-4+1.9j)^2 + (-4+1.9j)}\right) = 180 - 51.65 = 128.35$$

The system is seen requiring a phase lead of 128.55. The required pole and zero placement are then related as:
$\theta_t = \theta_P + \theta_Z = 128.35$

Thus, it may be deduced that the addition of a pole must result in a minimal increase in θ_t such that $\theta_Z < 180$. We therefore place the additional pole to the left-hand side of the desired pole location by offset **Γ** (**Figure 11**)

Relating the pole and zero positions to the reference frame at $x = Re\{-4+1.9j\}$:

$$\theta_Z = 128.35 + \tan^{-1}\left(\frac{Im\{-4+1.9j\}=1.9}{\Gamma}\right) \text{ , } \tan(180-\theta_Z) = \frac{Im\{-4+1.9j\}=1.9}{\sigma}$$

Thus, it follows that,

$$\sigma = \frac{1.9}{\tan(180 - 128.35 - \tan^{-1}(\frac{1.9}{\Gamma}))}$$

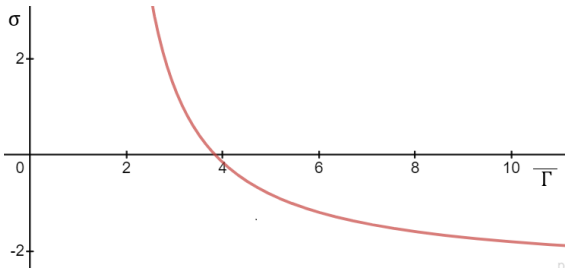

A plot of σ vs Γ indicates strong zero placement sensitivity for small values of Γ. This is because smaller Γ displacements contribute a larger $|\theta_P|$ which must then be offset by a larger θ_Z (and thus σ). A stable region exists where $\Gamma > 5$.

For a pole placement at $\Gamma = 5, s = -9$ the above relation yields $\sigma = 3.18, s = -0.82$ zero placement. This yields a controller transfer function as defined in Fig 5. Finally, the root locus gain is found as follows (using monic $q(s)$):

$$0.52\left(\frac{19.552}{6.8816}\right)k = \left|\frac{1}{q(s=-4+1.9j)}\right| = \left|\frac{1}{\frac{(s+0.82)}{(s+9)}\frac{1}{s\left(s+\frac{1}{6.8816}\right)}}\right|, k = 18.36, k(s) = 18.36\frac{(s+0.82)}{(s+9)},$$

The above derived controller $k(s)$ is known as a lead PD controller. A MATLAB simulation of the above derived controller (of **r2y**) was preformed using a step input.

```
s = tf("s");
G = 19.55/((6.882*s^2 + s));
K = 18.36 * ((s+0.82)/(s+9));
H = 0.52;
T = feedback(G*K*H,1);
step(T);
```

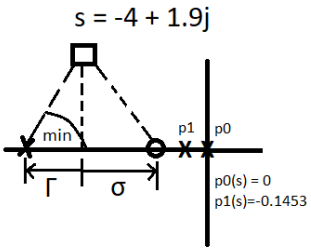

Figure 11. Pole/Zero offsets

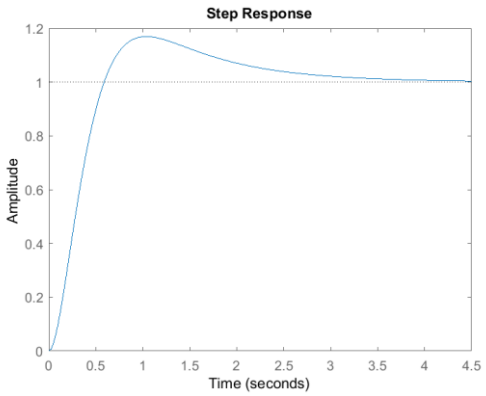

Figure 12. Step Response (r2y)

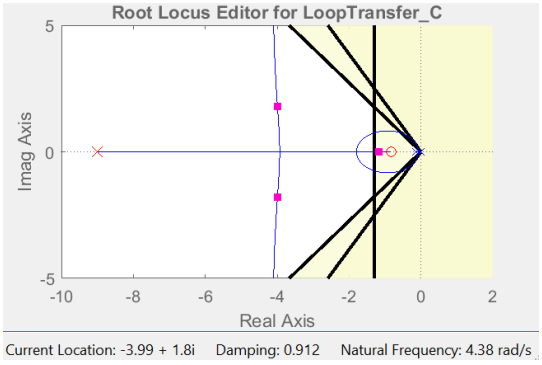

Figure 13. Controller validation

The resulting output shown in (**Figure 12**) satisfies both the %PO condition < 20% and t±2% condition < (0.5 * 6.8816) = 3.44s.

However, another important factor to consider was the **r2u** output response since the transfer function relating step input (r) to output (y) was modelled without the assumption of saturation of the control action u(t). Given our finite dynamic range [0,5V] and bias point of 2.5V a maximum 2.5V peak amplitude restriction was required.

A step response of **r2u (Figure 15)** of the closed loop transfer function was plotted and examined. A brief 0.2 sec saturation of 5% above the bias was observed near the mid-point of the control action. Model inaccuracy and component tolerances were within this range of uncertainty and so the model was accepted for implementation.

Despite our derived k(s) a PID controller, incorporating and integrator term, could also have been used. However, the redundancy added by an extra integrating term serves no significant advantage over the lead controller used as the main controller implementation.

5. Controller Implementation

Proportional Controller

A proportional controller, like any other feedback network, consists of a comparator element, a feedback path and a gain block, where $k(s)$ is purely scalar. Both the comparator, bias and gain blocks were implemented with op-amps.

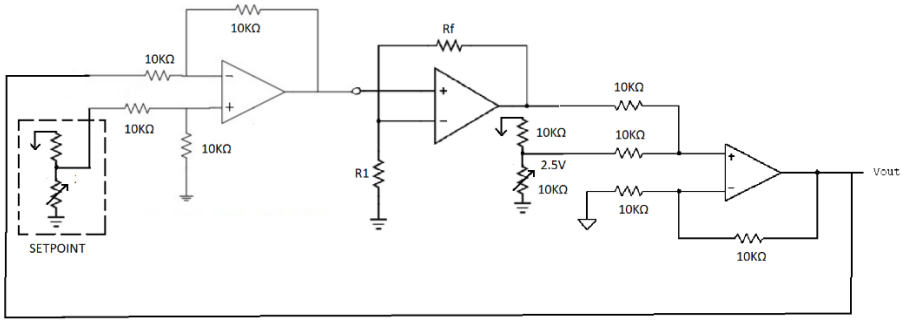

The controller gain k is defined as $\mathrm{k} = 1 + \frac{Rf}{\mathrm{R1}}$.

Since the proportional controller is not a pole effector (in the sense that a lead controller is), the response is constrained to that of figure 1, with increasing controller gain functioning to increase the natural frequency of the system, which is unwanted, thus a minimum value of k=2 is chosen. Set Rf = R1 =10k

Lead PD Controller

The lead controller derived as $k(s) = 18.36\frac{(s+0.82)}{(s+9)}$ needs practical implementation. The general form for a passive PD controller is given by:

$$\mathrm{k(s)} = \frac{1 + \mathrm{a}\tau\mathrm{s}}{1 + \tau\mathrm{s}}, \tau = \frac{CR_1R_2}{R_1 + R_2}, \mathrm{a} = \frac{R_1 + R_2}{R_2}$$

It follows that:

$$R_1 = R_2(a-1), R_2 = \frac{\mathrm{a}\tau}{C(\mathrm{a}-1)}$$

$$k(s) = 18.36\left(\frac{0.82}{9}\right)\frac{\left(1+\frac{1}{0.82}s\right)}{\left(1+\frac{1}{9}\right)}, \tau = \frac{1}{9} = 0.11, \mathrm{a} = 10.87, \text{ choose } \mathrm{C} = 100 * 10^{-6}\mathrm{F}$$

$$R_2 = \frac{\frac{1}{0.82}}{100 * 10^{-6}(10.87-1)} = 1.2K\Omega,\ R_1 = 1.2(10.87-1) = 11.8k\Omega$$

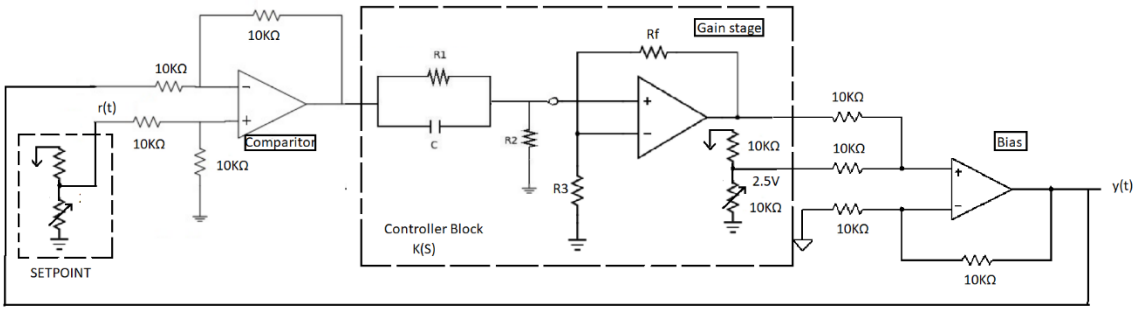

Where controller gain $\mathrm{k} = 1 + \frac{Rf}{\mathrm{R3}} = 1.67 \approx 2$.Thus we set $Rf = R3 = 1.2K\Omega$.Op-amps were powered with +-15V rails.

The response obtained from the controller above was similar to the simulated r2y output plotted on MATLAB. However, settling time was within a 20% error boundary which was eliminated by increasing the controller gain k to 4 without effecting the other system parameters significantly, such as %PO.

Tolerances were tested by using different component sets of the same value. No significant change in system performance was noted due to tolerances.

6. System Testing

The system performance of both controllers was characterized by plotting both the setpoint track and current position/altitude output against each other as well as the actuation output voltage using the software GUI interface for the simulator.

The performance of the controller was then characterized by the ability of helicopter to track changes in the setpoint as accurately as possible.

Performance metrics such as settling and rise times, peak overshoot and input/output disturbances were subsequently measured with input/output disturbance functionality being provided by the GUI interface allowing input disturbance for a set duration to be specified and applied.

In both types of controller, it was necessary to calibrate the DC bias point of the system. This involved placing the setpoint to its minimum and then adjusting the DC bias potentiometer until a reading of 2.5V was obtained in the software GUI sensor label.

Proportional Controller

The proportional controller in closed loop configuration did not produce satisfactory results and all user requirements specified for the project were not met during tests.

Increasing controller gain, had the effect of speeding up the response somewhat, but considerably increased the natural frequency response of the system which resulted in large amplitude variations in the helicopter's altitude.

Input disturbances applied to this type of controller resulted in a sudden increase in oscillation rate, and increased settling time. Overall the proportional controller did not have a stable and predictable response as required.

Lead Controller

Using the lead controller, however, produced significantly improved results. With the modified gain configuration (k=4), %PO and settling times were within requirement, with **Table IV**. summarizing the simulated vs realized performance specifications.

Parameter	Description	Realized	Simulated
A±2%	Steady state error	< 5%	< 2%
t±2%	Settling time	< 3s	< 3.2s
ζ	Damping ratio	Z> 0.85	Z> 0.9
%PO	Percent overshoot	< 15%	< 20%

Table IV. Values obtained for each set of readings.

Adjusting the gain parameter (k) seemed to affect the settling time t±2% with increases in k decreasing settling time and slightly increasing percent overshoot.

Input disturbances into the system resulted in a corrective action by the controller, with the controller producing a corrective action over time.

Steady state errors were observed to be within specification and a relation between the DC bias point, 2.5V nominal, and the steady state tracking error were observed. When the DC bias point was not aligned correctly, the deviation in steady state tracking error was seen to be proportional to the bias voltage error (differential).

Furthermore, it was observed that the output actuation, although saturating for a brief period as predicted by simulation had no impact on the nominal performance metrics. On the contrary, the control action for most of its actuation state from idle was observed to be robust and predictable.

7. Conclusion

Using the method of pole placement synthesis and root locus analysis a suitable controller has been designed with minor modification from its design model that achieves the full range of user specification as outlined in Fig 2.

The final controller achieves a closed loop performance as indicated in Fig 4. The response from its proportional controller model has been significantly improved, with settling times decreasing from approximately t±2%=60s to just under t±2%<3s as well as %PO figures decreasing from just over 90% to just under 15%.

Control actuation $u(t)$ is predictable, resulting in a smooth and controlled actuation signal

Thus, the advantage that a properly designed closed loop controller provides is significant.

Analysis of the so-called actuation 'cost' of the control system may be defined in terms of the signal power consumed over the duration of each step input or the total actuation signal energy.

A MATLAB script was written to calculate the energy in the r2u actuation response and is shown below.

```
s = tf("s");
G = 19.55/((6.882*s^2 + s));
K = 18.36 * ((s+0.82)/(s+9));
H = 0.52;
r2u = K/(1+G*K*H);
[x,t] = step(r2u);
energy = sum((abs(x).^2) * t(2) );
```

Figure 14. MATLAB energy calculation

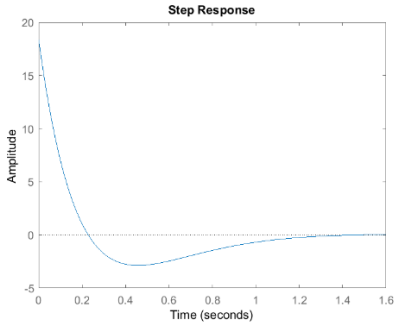

Figure 15. r2u actuation output

A value of approximately 23 Joules is obtained per actuation cycle. Of course, this is a theoretical number that does not take into account actuator saturation but serves as a figure of merit for the type of energy cycling in such a control system.

END